

SCIENTIFIC REPORTS



OPEN

Genomic Characteristics of Gender Dysphoria Patients and Identification of Rare Mutations in *RYR3* Gene

FuYang¹, Xiao-hai Zhu², Qing Zhang³, Ning-xia Sun³, Yi-xuan Ji³, Jin-zhao Ma¹, Bang Xiao¹, Hai-xia Ding³, Shu-han Sun¹ & Wen Li³

Gender dysphoria (GD) is characterized by an incongruence between the gender assigned at birth and the gender with which one identifies. The biological mechanisms of GD are unclear. While common genetic variants are associated with GD, positive findings have not always been replicated. To explore the role of rare variants in GD susceptibility within the Han Chinese population, whole-genome sequencing of 9 Han female-to-male transsexuals (FtMs) and whole-exome sequencing of 4 Han male-to-female transsexuals (MtFs) were analyzed using a pathway burden analysis in which variants are first collapsed at the gene level and then by Gene Ontology terms. Novel nonsynonymous variants in ion transport genes were significantly enriched in FtMs (P -value, $2.41E-10$; Fold enrichment, 2.8) and MtFs (P -value, $1.04E-04$; Fold enrichment, 2.3). Gene burden analysis comparing 13 GD cases and 100 controls implicated *RYR3*, with three heterozygous damaging mutations in unrelated FtMs and zero in controls ($P = 0.001$). Importantly, protein structure modeling of the *RYR3* mutations indicated that the R1518H mutation made a large structural change in the *RYR3* protein. Overall, our results provide information about the genetic basis of GD.

Gender dysphoria (GD), a controversial diagnostic class in the American Psychiatric Association's (APA) *Diagnostic Statistical Manual of Mental Disorders* (DSM) 5, causes persistent discomfort with one's biologic sex. There are many other terms currently in use to describe this condition, including gender identity disorder, transsexual and transgender. It is estimated that fewer than 1 in 10,000 adult natal males and 1 in 30,000 adult natal females experience GD¹. The etiology of GD is believed to be multifactorial, involving biological (including hormonal and genetic factors) and psychosocial factors^{1,2}. The brain is considered as the anatomical locus of gender identity^{3,4}. In human brains, there are region-specific dimorphisms with some structures larger in males (such as the hypothalamus and amygdala) and some larger in females (such as the caudate nucleus and hippocampus)⁵. However, it is still unclear what the role of these dimorphisms is in the development of GD. Heritability studies have demonstrated a genetic factor for the development of GD⁶. Recently, a twin study reported that 9 of 23 (39.1%) monozygotic female and male twins were concordant for GD. In contrast, none of the 21 same-sex dizygotic female and male twins were concordant for GD⁷. This indicates a role for genetic factors in the development of GD. A small number of candidate genes for GD have been studied, including the androgen receptor, estrogen receptor alpha, estrogen receptor beta, CYP17A1 and CYP19A1⁸⁻¹³. However, these results are rather mixed⁴. At present, no strong candidate gene has been identified that can account for the development of GD¹.

It is generally considered, based on the small sample size, that replication of positive findings focusing on common polymorphic variants is difficult¹⁴. This raises the question of whether "some heritability" of rare complex diseases is missed¹⁵. For a substantial portion of these diseases, determining their heritability requires a more comprehensive assessment of rare human variants^{16,17}. The emergence of next-generation sequencing platforms,

¹Department of Medical Genetics, Second Military Medical University, Shanghai, 200433, China. ²Department of Plastic Surgery, Changzheng Hospital, Second Military Medical University, Shanghai, 200433, China. ³Center of Reproductive Medicine, Shanghai Changzheng Hospital, Second Military Medical University, Shanghai, 200003, China. FuYang and Xiao-hai Zhu contributed equally to this work. Correspondence and requests for materials should be addressed to F.Y. (email: yangfusq1997@smmu.edu.cn) or S.-h.S. (email: shsun@vip.sina.com) or W.L. (email: lyliwen@sina.com)

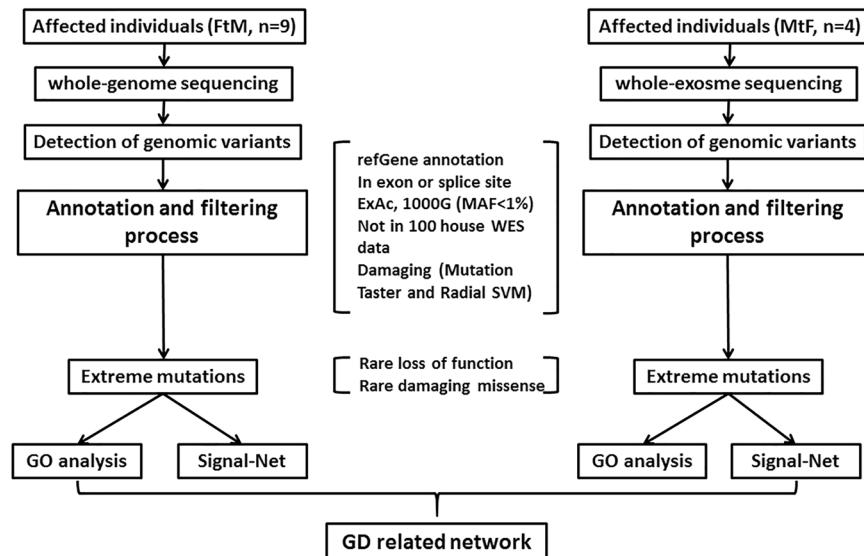


Figure 1. Flowchart for the exploration of disease genes in sporadic GD patients.

such as whole-genome sequencing (WGS) and whole-exome sequencing (WES), offers an unprecedented opportunity to identify the molecular causes of rare genetic diseases^{18–20}. Many studies have identified genes conferring risk for spinal deformity^{21,22}, schizophrenia²³ and autism²⁴ by applying WES in patients with no family history of these disorders or their related phenotypes.

We hypothesized that rare genetic variants are a major contributor to GD susceptibility. In the current pilot study, we employed a combined multistep approach to examine 9 female-to-male transsexuals (FtMs) using WGS and 4 male-to-female transsexuals (MtFs) using WES to identify rare variants associated with GD. These genetic and clinical studies of GD patients were restricted to the Chinese Han population. The present study suggests the value of next-generation sequencing platforms in revealing genetic mechanisms involved in the development of GD, but also highlights their limitations and the need for additional studies using larger patient and control sample sizes.

Results

We hypothesized that rare genetic variants are a major contributor to GD susceptibility. In the current pilot study, we employed a combined multistep approach to examine 9 FtMs using WGS and 4 MtFs using WES to identify rare variants associated with GD. Their mean age at sex reassignment surgery was 30.2 (± 4.3) years. None of them have a family history of GD, schizophrenia or related phenotypes. All subjects (FtMs and MtFs) were Han Chinese and diagnosed as early-onset GD. Other clinical and demographic characteristics of the included subjects are shown in Table S1. Raw data for the whole genome screen are shown in Table S2. A total of 632,000,316–904,682,628 reads were generated. The average map rate was 96.68%, and approximately 77.31–90.20 Gbp were aligned to the reference genome (hg19) with a mapping quality of Q20. The information from the whole exome screen is shown in Table S3. On average, 97.7% of the generated sequences aligned to the reference genome (hg19), and 97.7% of the targeted bases in each individual were assessed by ≥ 5 independent sequence reads. Only rare variants (defined as minor allele frequency [MAF] < 1% in 1000 Genome, ExAC) causing nonsense, splice-site, missense or insertion/deletion mutations were included in the analysis. Furthermore, we excluded variants found in our own in-house exomes ($n = 100$) from individuals with unrelated diseases. All the filtered rare variants were predicted to be disease-causing by the mutation prediction software MutationTaster and RadialSVM. This filtering strategy was selected to enrich for mutations that are rare and most likely to be deleterious (Fig. 1). A total of 401 non-synonymous SNVs covering 377 genes (no indels) were identified in FtMs (Table S4), and 283 non-synonymous SNVs and 20 exonic indels covering 275 genes were identified in MtFs (Table S5). Among the mutated genes in GD patients, *Ryanodine Receptor 3 (RYR3)*, which is a ryanodine receptor that functions to release calcium from intracellular storage for use in many cellular processes, was found to be recurrently mutated in three FtMs and zero in 100 controls (gene burden analysis, $P = 0.001$, Table 1). In addition, all the three *RYR3* variants were confirmed using Sanger sequencing (Fig. 2), and none of 275 ethnicity-matched controls (130 male and 145 female Han Chinese) carried these variants.

We further analyzed the biological function of the 377 FtM mutated and 275 MtF mutated genes using the DAVID functional classification tool (DAVID 6.7 <https://david-d.ncicrf.gov/summary.jsp>). For the 377 mutated genes in FtMs, the enriched GO terms were assigned to 67 clusters ranked by the biological significance of the gene groups based on GOTERM_BP_FAT (Table S6). Fifty-four genes included in the top cluster (enrichment score: 7.3) belong to 4 GO terms that are mainly involved in ion transport (Table S7). For the 275 mutated genes in MtFs, the enriched GO terms were assigned to 55 clusters ranked by the biological significance of the gene groups based on GOTERM_BP_FAT (Table S8). Twenty-six genes included in the top cluster (enrichment score: 2.1) belong to 5 GO terms that are mainly involved in ion transport (Table S7).

cDNA mutation*	Protein alteration	MutationTaster score	MutationTaster pred	RadialSVM score	RadialSVM pred	1000g_EAS	ExAC_EAS	Sample ID
c.4G>A	p. 2A>T	0.974	D	0.38	D	.	.	Patient 4 (FtM)
c. 4553G>A	p. 1518R>H	1	D	0.973	D	0.002	0.001	Patient 9 (FtM)
c. 8539A>G	p. 2847T>A	0.994	D	0.138	D	.	0.0031	Patient 6 (FtM)

Table 1. Summary of *RYR3* mutations in GD patients. *The accession number for *RYR3* is GenBank NM_001036.

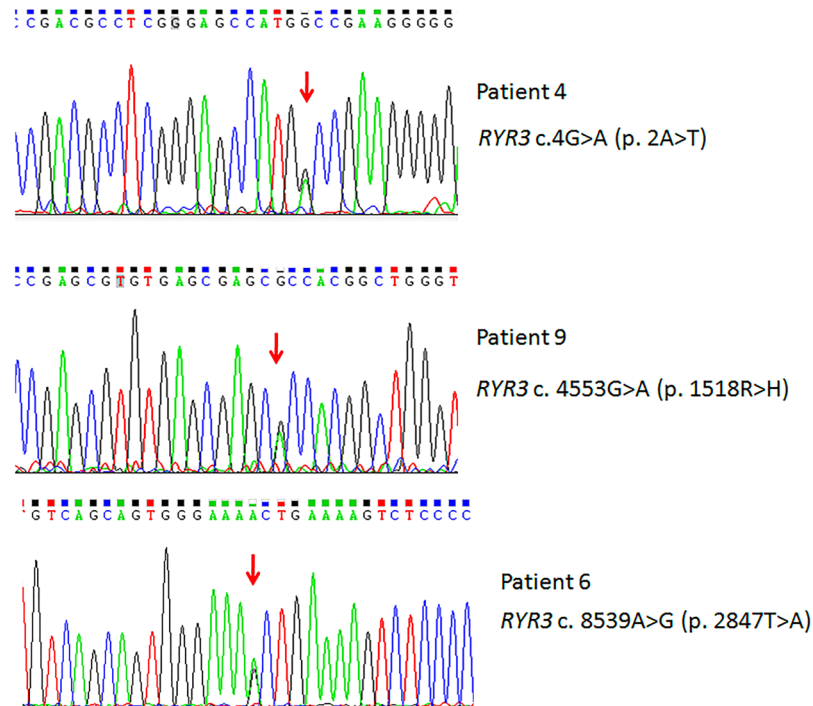


Figure 2. Heterozygotes *RYR3* mutations are identified in three FtMs (Patient 4, Patient 6, Patient 9). All mutations were verified by Sanger sequencing. Red arrows indicate the positions of point mutations.

Knowledge of molecular-level interactions between proteins has enabled the development of signal-net networks enriched for the 377 genes mutated in FtMs (Fig. 3A) or the 275 genes mutated in MtFs (Fig. 3B). The underlying connections were explored by MySQL 5.1.3 (Oracle, CA, USA) using experimentally verified interaction data from KEGG (<http://www.kegg.jp/kegg/pathway.html>). We found that the two networks (based on the mutated genes in FtMs and MtFs, respectively) encompass ion transport related modules. The ion transport-related module components in the FtM network (Fig. 3A) included 11 proteins: ITPR1, ITPR2, ITPR3, RYR2, RYR3, NNT, CACNB2, CTT1B, CPT2, PSEN2 and PLCG2. The ion transport-related module components in the MtF network (Fig. 3B) included 7 proteins: ITPR3, TRPM5, KCNB1, ATP2B2, CACNA1I, XCR1 and PLCG2.

GD is commonly thought to arise from a discrepancy between cerebral and genital sexual differentiation. We therefore examined the expression of ion transport-related module components in different anatomical regions of the brain across previously published microarray data sets using the GENEVESTIGATOR platform. The anatomy profile (Gene Atlas tool) results revealed strong *RYR3* expression in the hippocampus, associative striatum, frontal pole and caudate nucleus (signal intensity on Affymetrix Human Genome U133 Plus 2.0 Array >13), but low or medium signals in other regions of the brain (signal intensity on Affymetrix Human Genome U133 Plus 2.0 Array <13) (Fig. 4A). However, PLCG2 and ITPR3 were uniformly expressed in each brain region (Fig. 4; for PLCG2, 9 < signal intensity on Affymetrix Human Genome U133 Plus 2.0 Array < 12; for ITPR3, 10 < signal intensity on Affymetrix Human Genome U133 Plus 2.0 Array < 12).

Comparative modeling methods use structural templates that have the highest sequence homology with the target protein. Homologous proteins were identified by scanning the protein sequence of *Homo sapiens* *RYR3*, obtained from the ExPASy server, against 3D structures deposited in the Protein Data Bank using PSI-BLAST. The *Oryctolagus cuniculus* *RYR1* (PDB code: 3J8H) was a promising template with sequence identity of 64.6%

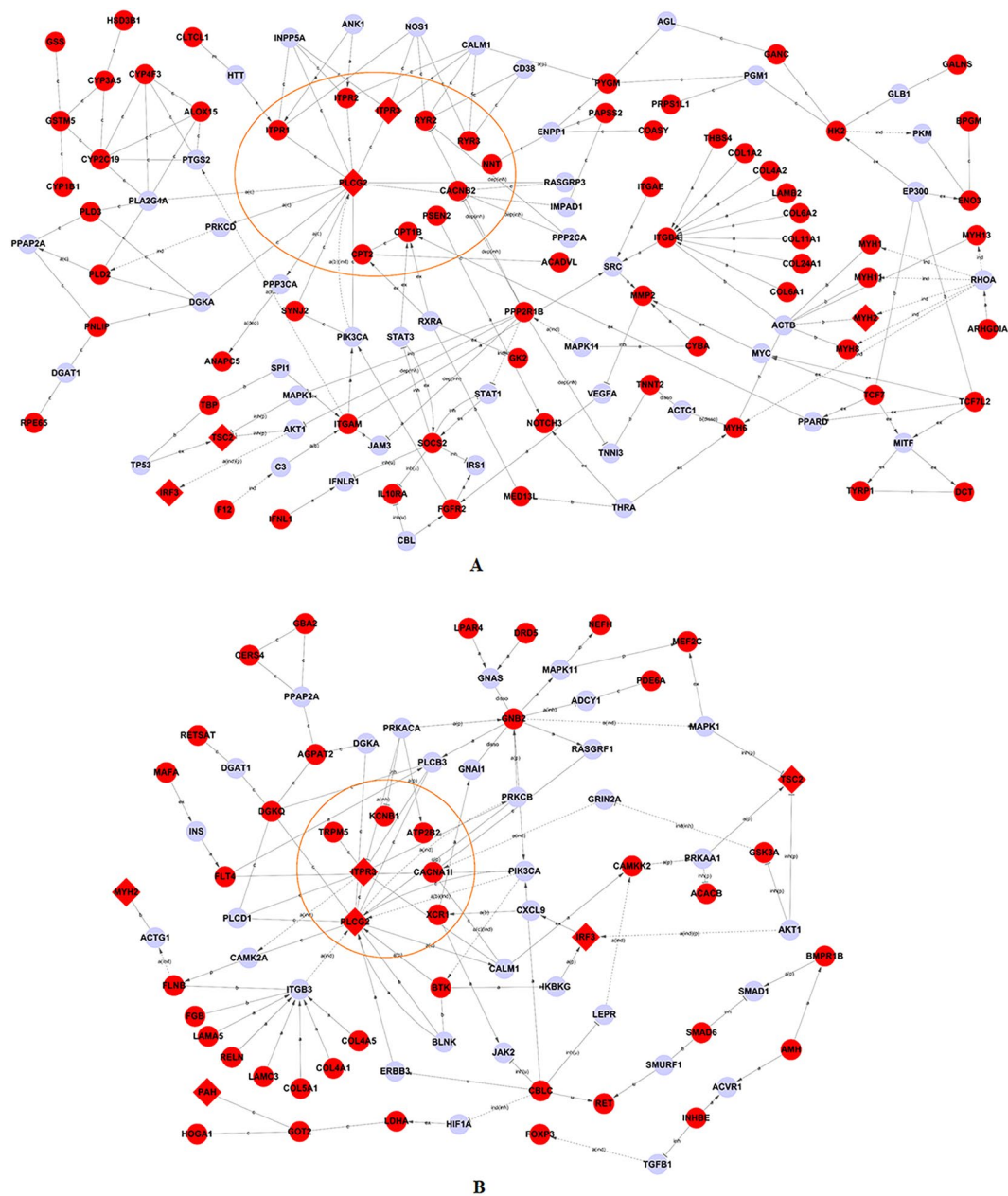


Figure 3. Functional analysis of the network containing identified rare and damaging mutations in GDs reveals enrichment for genes involved in ion transport. The network was algorithmically constructed using GeneSignalNetwork software (Genminix, Shanghai, China) based on the functional and biological connectivity of genes. The network is graphically represented as nodes (genes) and edges (the biological relationship between genes). Red nodes represent genes containing identified mutations in FtMs (A) and MtFs (B). The other nodes (light blue) are those that GeneSignalNetwork automatically includes because they are biologically linked to the studied genes based on evidence in KEGG. The genes in yellow circles participate in the process of ion transport.

and a good *E*-value (Fig. 5A). The PDB structure was loaded into MOE and the sequence alignment performed in MOE with the alignment constrained between the target and the template.

A model, based on the template using a single template alignment approach, was generated using MOE software as described in the methods section. Ten intermediate models were generated and the final model was taken as the Cartesian average of all the intermediate models. Then, the final model was submitted to global minimization using the energy minimize module of MOE (Fig. 5B). To evaluate the quality of the modeled structure, a geometric analysis was performed in MOE, including a Phi-Psi Plot, bond lengths, bond angles, and rotamers. The stereochemical quality of the protein backbone and side chains was evaluated using Ramachandran plots via Phi-Psi Plot analysis. In the Ramachandran plot, 95% of the residues of the RYR1-based model were in the allowed region, which indicates that the backbone dihedral angles φ and ψ in the final model were reasonably accurate.

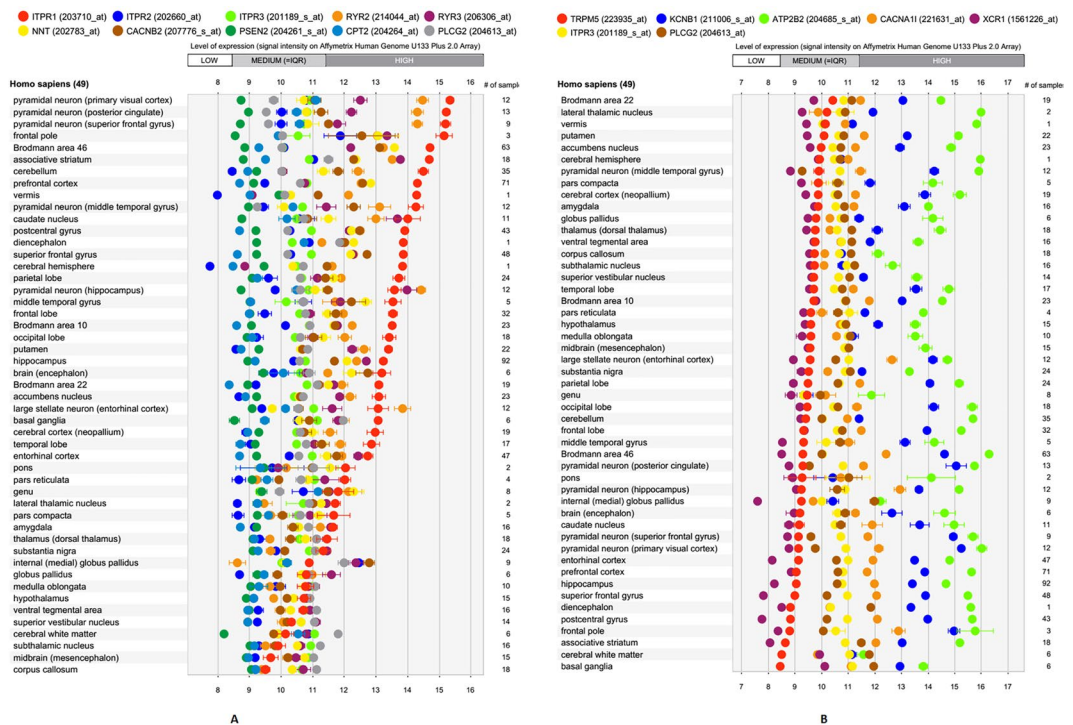


Figure 4. The relative expression levels of mutated ion transport genes in FtMs (A) and MtFs (B) in healthy brain tissue were identified using the GENEVESTIGATOR platform.

To obtain the stable structure, the homology model was minimized, followed by a manual mutation of p. 2A > T, p. 1518R > H and p. 2847T > A. MOE suggested possible changes in the molecular structure induced by these mutations. These mutations may introduce a new intramolecular hydrogen bond causing the structural changes. Of the three mutations, the p. 1518R > H mutation produced the largest structural change in the RYR3 protein. Figure 5D shows that the mutation caused three intramolecular hydrogen bonds to form between Met819, Gly1520, Trp1521 and His1518, which promotes structural changing that move the side chain of the His1518 from the outside to the inner side. In the wild-type RYR3 homology model, Arg1518 did not show any interactions with these residues. This phenomenon was not seen in the p. 2A > T and p. 2847T > A mutants (Fig. 5C and E). In both the wild-type and p. 2A > T mutant, residue Ala2 and Thr2 could form a hydrogen bond with Met1 (Fig. 5C). The length of the side chains for Ala and Thr are almost the same. In both the wild-type and p. 2847T > A mutant, a hydrogen bond is found either between Thr2847 and Ser2850 or Ala2847 and Ser2850. In p. 2A > T and p. 2847T > A mutants, the structural changes may not be obvious.

Discussion

It is widely accepted that genetic factors play key roles in the etiology of GD¹. In recent years, the association between GD and gene polymorphisms has been investigated^{8–13, 25, 26}. We investigated possible GD-associated pathogenic mutations by performing a WGS analysis of 9 FtMs and WES analysis of 4 MtFs. We identified heterozygous mutations of *RYR3* in three Han Chinese with GD. To the best of our knowledge, this is the first time that genotypic assessment by next generation sequencing has been applied to research GD. To use this new advanced technique of genetic analysis, it is best that the sample be homogeneous; therefore, all subjects (FtMs and MtFs) were Han Chinese and diagnosed as early-onset GD (Table S1).

Electrical activity in neurons requires a close functional coordination between plasmalemmal ion channels and ion transporters²⁷. Although ion channels have been studied intensively for several decades, research on ion transporters is in its infancy. For brain disorders such as Parkinson's disease, schizophrenia and depression the ion transporter system, being intertwined with many other signaling systems, plays a key role in pathogenesis and therapy^{28–31}. Studying the functions of these transporters may lead to major paradigm shifts in our understanding of the mechanisms underlying brain development and plasticity in health and disease. GD is thought to be a consequence of atypical cerebral sexual differentiation⁴. The observed differences between GD patients and controls indicate that gender dysphoria may be associated with changes in multiple structures and involve a network (rather than a single nodal area)^{32–35}. There is evidence indicating the important role of sex hormones in the sexual differentiation of brain^{36, 37}. It is also believed that the foetal brain may develop into a male brain under the influence of testosterone, or into a female brain in the absence of this hormone³⁸. Thus, GD may result from a discrepancy between sexual brain and genital differentiation caused by genetic or hormonal deviations⁴. Ryanodine receptors are intracellular calcium-release channels found on the endoplasmic reticulum of all cells. *RYR3* is highly expressed in the hippocampus, associative striatum, frontal pole and caudate nucleus (Fig. 3A). During the physiological processes of sexual brain development, the intracellular calcium homeostasis may be

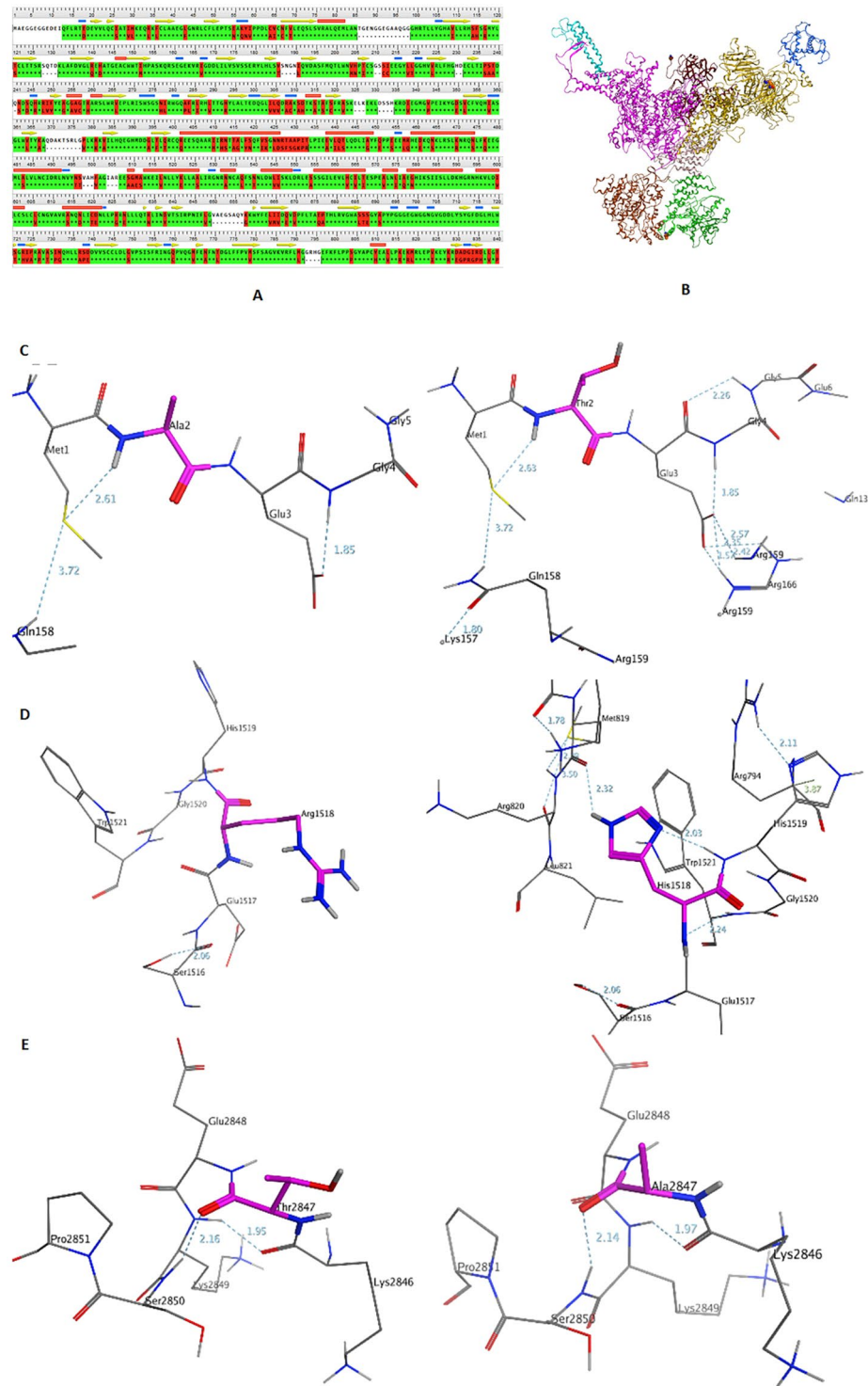


Figure 5. Analysis of conformational changes in mutant proteins. (A) The sequence alignment (part of the whole sequence) between *Homo sapiens* RYR3 (up) and *Oryctolagus cuniculus* RYR1 (down). The sequence identity is approximately 64.6%. (B) The homology model of the RYR3 receptor obtained by using MOE. The three mutation sites: A2, R1518 and T2847 are highlighted in the ball mode. Localized interactions at the three mutation sites: A2, R1518 and T2847. (left: C,D, and E) shows the original structures, T2, H1518 and A2847. (right: C,D, and E) shows the mutated structures. The three core residues are highlighted in purple and the hydrogen bonds formed around them are show.

largely regulated by RYR3. Mutations of RYR3 may cause imbalance of intracellular calcium homeostasis, leading to impairment of neuronal function. Although our data show that specific ion transporter genes, including RYR3, may contribute to GD risk, it is equally striking to consider the combined impact of variants in ion transporter genes as a class on GD susceptibility. The majority of genes within this group may contribute to GD risk, but the risk may also increase proportionally with the number of variants within an individual. Demonstration of the collective effect of multiple rare variants across ion transporter genes on GD fits with a polygenic burden disease model that was previously described^{22,39}.

In summary, our results provide information about the genetic basis of GD. This study also has some limitations. First, because the subjects were of Han Chinese origin, the results cannot be generalized to all populations. Second, the study was performed in only 9 FtMs and 4 MtFs. Therefore, similar studies using larger numbers of patients are necessary.

Materials and Methods

Subjects. All the patients were diagnosed according to the Diagnostic and Statistical Manual of Mental Disorders, fifth edition (DSM-5) criteria for GD in adults. All blood samples were collected between March 2012 and March 2016 from GD patients before sex reassignment surgery. Clinical and demographic characteristics of the included subjects are shown in Table S1. The study was approved by the Second Military Medical University (Shanghai, China) ethics committee and written informed consent was obtained from all participating patients. The methods were carried out in accordance with the principles stated in the Declaration of Helsinki.

WGS and WES. Our analysis included WGS data from 9 FtMs and WES data from 4 MtFs. For WGS, DNA was extracted from blood, and 500 bp insert libraries were prepared according to the protocol provided by Illumina. The libraries were sequenced on HiSeq X platforms with paired-end reads of 101 bp. For sequence data analysis, read pairs were mapped with the Burrows-Wheeler Aligner (BWA), and the resulting files were converted to the pileup format via SAMtools⁴⁰. After PCR duplications were removed, single nucleotide variations (SNVs) and indels were identified. Four MtFs were selected for WES. Whole-exome capture by the SureSelect Human All Exon Kit (Agilent) and high-throughput sequencing by the HiSeq. 2000 sequencer (Illumina Inc.) were conducted by Genergy (Shanghai, China).

Bioinformatics Analysis. To explore the potential biological functions of the mutated genes identified in FtMs and MtFs, the genes were uploaded to DAVID 6.7⁴¹ for functional annotation clustering analysis based on GO terms (GOTERM_BP_FAT).

The GeneSignalNetwork analysis was performed by Genminix (Shanghai, China) as previously described⁴². First, an interactions repository derived from KEGG was constructed. Using GeneSignalNetwork, we obtained a given protein's upstream or downstream interactions through the whole KEGG Pathway database. We connected two gene nodes when their corresponding proteins were either directly or indirectly connected by a linker gene in the interaction network. The network for each gene was measured by counting the number of upstream and downstream genes or binding genes, which were expressed as in-degree and out-degree or degree, respectively (More information can be found in this link: <http://college.gcbi.com.cn/fangfaxue/676.jhtml>).

For in silico identification of the expression levels of genes in different anatomical regions of the brain, we used the Signature tool from the GENEVESTIGATOR search engine⁴³. For analysis, we selected data sets from the Affymetrix Human Genome U133 Plus2.0 Array platform. Then, knowledge-driven selection of healthy brain microarray data sets was performed.

Homology Modeling. The target sequence of wild-type *Homo sapiens* Ryanodine receptor 3 (RYR3) was selected as the input for homology modeling. The crystal structure of the Ryanodine receptor 1 from *Oryctolagus cuniculus* (PDB code: 3J8H, resolution: 3.8 Å) was downloaded from the Protein Data Bank for use as the template. The homology modeling process was performed using the Molecular Operating Environment package, version 2015.1001 (Chemical Computing Group, <http://www.chemcomp.com>). Ten independent intermediate models were built by permutational selection of various loop candidates and side-chain rotamers. The intermediate model that scored best according to the GB/VI scoring function was chosen as the final model.

In Silico Mutation Modeling. To analyze the possible changes in the molecular structure, in silico mutations were performed based on the wild-type structure obtained from the homology modeling. The mutations in RYR3 (A2T, R1518H, and T2847A) were modeled using the Protein Builder application in MOE. The stable structures of the wild-type and mutant RYR3 proteins were obtained by minimization in MOE. Amber10:EHT was used as the force field. The intramolecular interactions and structural changes were analyzed both in the wild-type and mutant RYR3 proteins.

References

- Zucker, K. J., Lawrence, A. A. & Kreukels, B. P. Gender Dysphoria in Adults. *Annu Rev Clin Psychol* **12**, 217–47 (2016).
- Fuss, J., Auer, M. K. & Briken, P. Gender dysphoria in children and adolescents: a review of recent research. *Curr Opin Psychiatry* **28**, 430–4 (2015).
- Bao, A. M. & Swaab, D. F. Sexual differentiation of the human brain: relation to gender identity, sexual orientation and neuropsychiatric disorders. *Front Neuroendocrinol* **32**, 214–26 (2011).
- Smith, E. S., Junger, J., Derntl, B. & Habel, U. The transsexual brain—A review of findings on the neural basis of transsexualism. *Neurosci Biobehav Rev* **59**, 251–66 (2015).
- Goldstein, J. M. *et al.* Normal sexual dimorphism of the adult human brain assessed by *in vivo* magnetic resonance imaging. *Cereb Cortex* **11**, 490–7 (2001).
- Coolidge, F. L., Thede, L. L. & Young, S. E. The heritability of gender identity disorder in a child and adolescent twin sample. *Behav Genet* **32**, 251–7 (2002).

7. Heylens, G. *et al.* Gender identity disorder in twins: a review of the case report literature. *J Sex Med* **9**, 751–7 (2012).
8. Cortes-Cortes, J. *et al.* Genotypes and Haplotypes of the Estrogen Receptor alpha Gene (ESR1) Are Associated With Female-to-Male Gender Dysphoria. *J Sex Med* **14**, 464–472 (2017).
9. Fernandez, R. *et al.* The (CA)_n polymorphism of ERbeta gene is associated with FtM transsexualism. *J Sex Med* **11**, 720–8 (2014).
10. Fernandez, R. *et al.* Association study of ERbeta, AR, and CYP19A1 genes and MtF transsexualism. *J Sex Med* **11**, 2986–94 (2014).
11. Hare, L. *et al.* Androgen receptor repeat length polymorphism associated with male-to-female transsexualism. *Biol Psychiatry* **65**, 93–6 (2009).
12. Henningson, S. *et al.* Sex steroid-related genes and male-to-female transsexualism. *Psychoneuroendocrinology* **30**, 657–64 (2005).
13. Ujike, H. *et al.* Association study of gender identity disorder and sex hormone-related genes. *Prog Neuropsychopharmacol Biol Psychiatry* **33**, 1241–4 (2009).
14. Visscher, P. M., Brown, M. A., McCarthy, M. I. & Yang, J. Five years of GWAS discovery. *Am J Hum Genet* **90**, 7–24 (2012).
15. Manolio, T. A. *et al.* Finding the missing heritability of complex diseases. *Nature* **461**, 747–53 (2009).
16. Le Scouarnec, S. *et al.* Testing the burden of rare variation in arrhythmia-susceptibility genes provides new insights into molecular diagnosis for Brugada syndrome. *Hum Mol Genet* **24**, 2757–63 (2015).
17. Mancuso, N. *et al.* The contribution of rare variation to prostate cancer heritability. *Nat Genet* **48**, 30–5 (2016).
18. Auer, P. L. *et al.* Guidelines for Large-Scale Sequence-Based Complex Trait Association Studies: Lessons Learned from the NHLBI Exome Sequencing Project. *Am J Hum Genet* **99**, 791–801 (2016).
19. Chong, J. X. *et al.* The Genetic Basis of Mendelian Phenotypes: Discoveries, Challenges, and Opportunities. *Am J Hum Genet* **97**, 199–215 (2015).
20. Hastings, R. *et al.* Combination of Whole Genome Sequencing, Linkage, and Functional Studies Implicates a Missense Mutation in Titin as a Cause of Autosomal Dominant Cardiomyopathy With Features of Left Ventricular Noncompaction. *Circ Cardiovasc Genet* **9**, 426–435 (2016).
21. Buchan, J. G. *et al.* Rare variants in FBN1 and FBN2 are associated with severe adolescent idiopathic scoliosis. *Hum Mol Genet* **23**, 5271–82 (2014).
22. Haller, G. *et al.* A polygenic burden of rare variants across extracellular matrix genes among individuals with adolescent idiopathic scoliosis. *Hum Mol Genet* **25**, 202–9 (2016).
23. Xu, B. *et al.* Exome sequencing supports a de novo mutational paradigm for schizophrenia. *Nat Genet* **43**, 864–8 (2011).
24. Liu, L. *et al.* Analysis of rare, exonic variation amongst subjects with autism spectrum disorders and population controls. *PLoS Genet* **9**, e1003443 (2013).
25. Bentz, E. K. *et al.* A polymorphism of the CYP17 gene related to sex steroid metabolism is associated with female-to-male but not male-to-female transsexualism. *Fertil Steril* **90**, 56–9 (2008).
26. Fernandez, R. *et al.* The CYP17 MspA1 Polymorphism and the Gender Dysphoria. *J Sex Med* **12**, 1329–33 (2015).
27. Ranade, S. S., Syeda, R. & Patapoutian, A. Mechanically Activated Ion Channels. *Neuron* **87**, 1162–79 (2015).
28. Jaggi, A. S., Kaur, A., Bali, A. & Singh, N. Expanding Spectrum of Sodium Potassium Chloride Co-transporters in the Pathophysiology of Diseases. *Curr Neuropharmacol* **13**, 369–88 (2015).
29. Kumar, P., Kumar, D., Jha, S. K., Jha, N. K. & Ambasta, R. K. Ion Channels in Neurological Disorders. *Adv Protein Chem Struct Biol* **103**, 97–136 (2016).
30. Pavlovicova, M., Lacinova, L. & Dremencov, E. Cellular and molecular mechanisms underlying the treatment of depression: focusing on hippocampal G-protein-coupled receptors and voltage-dependent calcium channels. *Gen Physiol Biophys* **34**, 353–66 (2015).
31. Yang, Y. C., Tai, C. H., Pan, M. K. & Kuo, C. C. The T-type calcium channel as a new therapeutic target for Parkinson's disease. *Pflugers Arch* **466**, 747–55 (2014).
32. Guillamon, A., Junque, C. & Gomez-Gil, E. A Review of the Status of Brain Structure Research in Transsexualism. *Arch Sex Behav* **45**, 1615–48 (2016).
33. Manzouri, A., Kosidou, K. & Savic, I. Anatomical and Functional Findings in Female-to-Male Transsexuals: Testing a New Hypothesis. *Cereb Cortex* **27**, 998–1010 (2017).
34. Savic, I. & Arver, S. Sex dimorphism of the brain in male-to-female transsexuals. *Cereb Cortex* **21**, 2525–33 (2011).
35. Soleman, R. S. *et al.* Oestrogens are Not Related to Emotional Processing: a Study of Regional Brain Activity in Female-to-Male Transsexuals Under Gonadal Suppression. *Cereb Cortex* **26**, 510–6 (2016).
36. Witte, A. V., Savli, M., Holik, A., Kasper, S. & Lanzenberger, R. Regional sex differences in grey matter volume are associated with sex hormones in the young adult human brain. *Neuroimage* **49**, 1205–12 (2010).
37. McCarthy, M. M. *et al.* The epigenetics of sex differences in the brain. *J Neurosci* **29**, 12815–23 (2009).
38. Savic, I., Garcia-Falgueras, A. & Swaab, D. F. Sexual differentiation of the human brain in relation to gender identity and sexual orientation. *Prog Brain Res* **186**, 41–62 (2010).
39. Purcell, S. M. *et al.* A polygenic burden of rare disruptive mutations in schizophrenia. *Nature* **506**, 185–90 (2014).
40. Van, K. *et al.* Genome-wide SNP discovery in mungbean by Illumina HiSeq. *Theor Appl Genet* **126**, 2017–27 (2013).
41. Huang da, W., Sherman, B. T. & Lempicki, R. A. Systematic and integrative analysis of large gene lists using DAVID bioinformatics resources. *Nat Protoc* **4**, 44–57 (2009).
42. Ni, D. *et al.* Downregulation of FOXO3a promotes tumor metastasis and is associated with metastasis-free survival of patients with clear cell renal cell carcinoma. *Clin Cancer Res* **20**, 1779–90 (2014).
43. Hruz, T. *et al.* Genevestigator v3: a reference expression database for the meta-analysis of transcriptomes. *Adv Bioinformatics* **2008**, 420747 (2008).

Acknowledgements

We thank all subjects and their families for participating in this study, and the local coordinators who helped facilitate sample collection and processing. This work was supported by National Natural Science Foundation of China (Grant No. 81472691).

Author Contributions

F.Y. and S.H.S conceived of and designed the experiments. W.L. and X.H.Z coordinated clinical sample collection and provided clinical interpretation. F.Y., Q.Z., N.X.S, Y.X.J., J.Z.M and B.X. performed the experiments. F.Y. analysed the data. F.Y. drafted the manuscript. All authors reviewed the manuscript. This work was supported by National Natural Science Foundation of China (Grant No. 81472691).

Additional Information

Supplementary information accompanies this paper at doi:10.1038/s41598-017-08655-x

Competing Interests: The authors declare that they have no competing interests.

Publisher's note: Springer Nature remains neutral with regard to jurisdictional claims in published maps and institutional affiliations.



Open Access This article is licensed under a Creative Commons Attribution 4.0 International License, which permits use, sharing, adaptation, distribution and reproduction in any medium or format, as long as you give appropriate credit to the original author(s) and the source, provide a link to the Creative Commons license, and indicate if changes were made. The images or other third party material in this article are included in the article's Creative Commons license, unless indicated otherwise in a credit line to the material. If material is not included in the article's Creative Commons license and your intended use is not permitted by statutory regulation or exceeds the permitted use, you will need to obtain permission directly from the copyright holder. To view a copy of this license, visit <http://creativecommons.org/licenses/by/4.0/>.

© The Author(s) 2017